

Autophagy induced by valproic acid is associated with oxidative stress in glioma cell lines

Jun Fu, Cui-Jie Shao, Fu-Rong Chen, Ho-Keung Ng, and Zhong-Ping Chen

State Key Laboratory for Cancer Research in Southern China, Department of Neurosurgery/Neuro-Oncology, Cancer Center, Sun Yat-Sen University, Guangzhou, People's Republic of China (J.F., C.-J.S., F.-R.C., Z.-P.C.); Department of Anatomical & Cellular Pathology, The Chinese University of Hong Kong, Hong Kong, People's Republic of China (H.-K.N.)

Autophagy represents an alternative tumor-suppressing mechanism that overcomes the dramatic resistance of malignant gliomas to radiotherapy and proapoptotic-related chemotherapy. This study reports that valproic acid (VPA), a widely used anti-epilepsy drug, induces autophagy in glioma cells. Autophagy, crucial for VPA-induced cell death, is independent of apoptosis, even though apoptotic machinery is proficient. Oxidative stress induced by VPA occurs upstream of autophagy. Oxidative stress also activates the extracellular signal-regulated kinase 1/2 (ERK1/2) pathway, whereas blocking this pathway inhibits autophagy and induces apoptosis. VPA-induced autophagy cannot be alleviated by inositol, suggesting a mechanism different from that for lithium. Moreover, VPA potentiates autophagic cell death, but not apoptosis, when combined with other autophagy inducers such as rapamycin, Ly294002, and temozolomide in glioma cells both in vitro and in vivo, which may warrant further investigation toward possible clinical application in patients with malignant gliomas.

Keywords: autophagy, glioma, oxidative stress, valproic acid

Malignant gliomas account for approximately 50% of primary tumors in the brain. Even when a combination of surgery, chemotherapy, and radiotherapy is used, the median survival time of patients with glioblastoma multiforme (GBM), the most malignant type of glioma, is still <1 year from diagnosis.¹ Resistance to apoptosis, a characteristic of

many cancers, especially malignant glioma, underlies not only tumorigenesis but also the inherent resistance of cancer cells to radiotherapy and chemotherapy.² Therefore, novel strategies are essential to improve prognosis of the patients.

Increasing evidence obtained in many model systems, both in vitro and in vivo, supports the hypothesis that a variety of cell death programs may be triggered in distinct circumstances. Autophagy, also known as programmed cell death type II, represents an alternative tumor-suppressing mechanism to overcome, at least partly, the dramatic resistance of many cancers to radiotherapy and proapoptotic-related chemotherapy.² Unlike apoptosis, which is a caspase-dependent process characterized by nuclear condensation and fragmentation but without major ultrastructural changes in cytoplasmic organelles, autophagy is a caspase-independent process characterized by the accumulation of autophagic vacuoles in the cytoplasm accompanied by extensive degradation of organelles, such as mitochondria and polyribosomes, and the endoplasmic reticulum, which precedes the destruction of the nucleus.³ However, autophagy may also be important in the regulation of cancer development as well as progression and in determining the response of tumor cells to anticancer therapy. Therefore, the role of autophagy is complicated and may, depending on the circumstances, have diametrically opposite consequences for the tumor.⁴

Manipulation of autophagy could have the potential to improve anticancer therapeutics. A number of studies have reported that autophagy, or autophagic cell death, can be activated in gliomas, in response to various anticancer therapies. Temozolomide (TMZ), a DNA-alkylating agent, can induce autophagy, but not apoptosis, in malignant glioma cells,⁵ and has demonstrated real therapeutic benefits in apoptosis-resistant GBM patients.⁶ Rapamycin, an inhibitor of the mammalian target of rapamycin (mTOR), can induce autophagy

Received July 30, 2008; accepted June 9, 2009.

Corresponding Author: Zhong-Ping Chen, Cancer Center, Sun Yat-Sen University Guangzhou, Guangdong 510060, People's Republic of China (chenzp57@mail.sysu.edu.cn).

in, as well as suppress the proliferation of, malignant glioma cells.⁷ Thus, novel successes in the fight against glioblastomas might be achieved by a combination of proautophagic drugs, such as TMZ, with inhibitors of mTOR, class IPI3K, or Akt as adjuvant chemotherapies.

Valproic acid (2-propylpentanoic acid, [VPA]) is a branched short-chain fatty acid and has widely been used in the management of various types of epilepsy for decades. VPA has been identified as a potent selective histone deacetylase inhibitor, which induces cellular differentiation, growth arrest, and apoptosis in gliomas and other types of cancers.⁸ Other studies reported that VPA induces growth arrest, apoptosis, and senescence in medulloblastoma and glioma cell lines by increasing histone hyperacetylation and regulating expression of p21Cip1, CDK4, and c-Myc.^{9–11} Although proapoptotic machinery was reported to be activated after exposure to VPA, other mechanisms may also be involved. Schwartz et al.¹² reported that VPA induces nonapoptotic cell death in multiple myeloma cell lines. Nevertheless, VPA was also proven to exert cytoprotection functions and suppress apoptosis in human SY5Y neuroblastoma cells.¹³ Michaelis et al.¹⁴ showed that VPA induces extracellular signal-regulated kinase 1/2 (ERK 1/2) activation and inhibits apoptosis in endothelial cells. However, the mechanisms underlying these effects of VPA in malignant gliomas remain poorly understood.

In this study, we investigated the role of autophagy in VPA-induced cytotoxicity and examined possible mechanisms of VPA-induced autophagy in glioma cell lines.

Patients and Methods

Glioma Cell Lines

Human glioma cell lines such as U87MG, SF295, and T98G were used in this study. The cells were cultured in Dulbecco's modified Eagle's medium supplemented with 10% fetal bovine serum (Hyclone, Logan, UT, USA), 4 mM glutamine, 100 U/mL penicillin, and 100 µg/mL streptomycin.

Reagents

Valproic acid, dansyl monodacaverin (MDC), propidium iodide (PI), *N*-acetylcysteine (NAC), pan-caspase inhibitor Z-VAD-fmk (zVAD), rapamycin, Ly294002, MEK1 inhibitor PD98059, H₂O₂, inositol, and 3-methyladenosine (3-MA) were purchased from Sigma Chemical Co. (St. Louis, MO). JC-1, 2',7'-dichlorodihydrofluorescein diacetate (H₂DCF), and mitotracker red CMXRos (MTR) were purchased from Molecular Probe (Eugene, OR, USA). Microtubule-associated protein 1-light chain 3 (MAP1-LC3), Beclin 1, and cleaved caspase-3 (p17) antibodies were obtained from Santa Cruz Biotechnology (Santa Cruz, CA, USA). ERK1/2 and phospho-ERK1/2 monoclonal antibodies were obtained from Cell Signaling Technology (Danvers, MA, USA).

Plasmid and Transfection

The vector pEGFP-hLC3 was constructed by inserting human MAP1-LC3 in pEGFP plasmid as described previously.¹⁵ The plasmid was purchased from ADDGENE plasmid sharing service (Cambridge, MA, USA). Transfection of glioma cells with pEGFP-hLC3 was performed using FuGene 6 transfection reagent (Roche Applied Science, Mannheim, Germany) according to the manufacturer's instruction. To quantify autophagic cells after drug treatment, we counted the number of autophagic cells demonstrated by GFP-LC3 dots (≥ 10 dots/cell) among 200 GFP-positive cells.

Cytotoxicity Assay

The cytotoxic effect of VPA on glioma cell lines was determined using a Trypan blue dye-exclusion assay as described previously.⁵ Tumor cells were seeded at 5×10^3 cells/well (0.5 mL) in 24-well flat-bottomed plates and incubated overnight. After exposure to VPA in various concentrations for 96 h, the cells were trypsinized and the number of viable cells was counted. The viability of untreated cells was regarded as 100%. For coinubation with TMZ, a single concentration of VPA (0.5, 1.0, or 1.5 mM) and different concentrations of TMZ ranging from 6.25 to 400 µM were added to cells and incubations carried out for 96 h. The IC₅₀ value was calculated with SPSS 10.0 statistical software.

Cell Cycle Analysis

Cell cycle analysis was performed as described previously.⁵ Briefly, after serum deprivation for 36 h, glioma cells were treated with or without 1.0 mM VPA for another 96 h. Cells were trypsinized, fixed by 70% ethanol overnight, and stained by Cellular DNA Flow Cytometric Analysis Reagent Set (Becton Dickinson, San Jose, CA, USA). DNA content was analyzed by the FACScans. Data were analyzed by Cell Quest software (Becton Dickinson).

Electron Microscopy Observation

To morphologically demonstrate the induction of autophagy in treated tumor cells, we performed an ultrastructural analysis as described previously.⁵ Glioma cells treated with or without 1.0 mM VPA for 96 h were fixed with ice-cold glutaraldehyde (2% in 0.1 M cacodylate buffer, pH 7.4) for 30 min. After fixation, the samples were postfixed in 1% OsO₄ in the same buffer for 1 h and then subjected to the electron microscopic analysis. Representative areas were chosen for ultrathin sectioning and viewed with a Philips EM 400 transmission electron microscope at an accelerating voltage of 80 kV.

MDC Incorporation Assay

Dansyl monodacaverin incorporation was quantified using procedures previously described.¹⁶ Cells were

incubated with 0.05 mM MDC in phosphate-buffered saline (PBS) at 37°C for 10 min. After incubation, cells were washed four times with PBS and collected in 10 mM Tris-HCl, pH 8.0, containing 0.1% Triton X-100. Intracellular MDC was measured (excitation wavelength 380 nm, emission filter 525 ± 20 nm) in a CytoFluor plate reader. To normalize the measurements to the number of cells present in each well, a solution of ethidium bromide was added to a final concentration of 0.2 mM and DNA fluorescence was measured (excitation wavelength 530 nm, emission filter 590 ± 40 nm). The MDC incorporated was expressed as specific activities (fold to control). MDC-staining autophagic vacuoles were visualized under a Leica DMIRE2 inverted confocal microscope.

Apoptosis Detection Assay

Apoptosis of VPA-treated tumor cells was detected using an annexin V-FITC kit (Biovision, Inc., California, USA), according to the manufacturer's instructions. Briefly, cells were plated on poly-lysine-coated cover slides and treated by VPA alone or in combination. After treatment, the inverted phosphatidylserine in the outer membrane of apoptotic cells was labeled with a fluorescent isothiocyanate (FITC)-labeled annexin V. After fixing with 4% paraformaldehyde and counterstaining with DAPI, the cells were examined under an Olympus BX61 fluorescence microscope. Pictures were scanned with a DP71 CCD digital camera. Five hundred cells were analyzed for each sample. Each experiment was repeated three times.

Mitochondrial Membrane Potential Assay

Mitochondrial membrane potential (MMP) was measured using the mitochondrial-specific dual-fluorescence probe, JC-1, based on the method described previously.¹⁷ Glioma cells were treated with VPA at different concentrations for 96 h. After treatment, the medium was removed and replaced with 10 µg/mL of JC-1 in culture media for 10 min followed by two washes with PBS. A CytoFluor plate reader (excitation wavelength 485 nm, slit width 20 nm) was used to monitor the fluorescence intensities for the monomer and the aggregated JC-1 molecules (emission wavelengths 520 nm, slit width of 25 nm, 580 nm slit width of 30 nm, respectively). Results were expressed as fluorescence ratio (580/530 nm).

Detection of Intracellular Reactive Oxygen Species

Intracellular reactive oxygen species (ROS) was detected by means of an oxidation-sensitive fluorescent probe (H₂DCF) as described previously.¹⁷ After drug treatment for 96 h, the cells were washed twice in PBS and then intracellular fluorescence was measured (excitation wavelength 485 nm, emission filter 530 nm) in a CytoFluor plate reader. DCF fluorescence was defined as an arbitrary unit.

Immunofluorescence Staining

Cells were cultured on the coverslips precoated with poly-lysine. After various treatment with drugs, the cells were fixed in 4% paraformaldehyde, permeated with 0.25% Triton X-100, blocked with 3% normal goat serum, stained with first antibody overnight, and labeled with a goat anti-mouse or goat anti-rabbit IgG conjugated with FITC (Santa Cruz, CA, USA). The cells were counterstained with Vectashield sealant containing 4',6-diamidino-2-phenylindole (DAPI) (Vector Laboratories, California, USA) and examined under an Olympus BX61 fluorescence microscope. Pictures were scanned with a DP71 CCD digital camera.

Western Blot Analysis

Cells were washed in cold PBS and lysed in a radio-immuno precipitation assay (RIPA) buffer containing 50 mM Tris-HCl, pH 7.4, 150 mM NaCl, 1 mM Phenylmethanesulfonyl fluoride (PMSF), 1 mM Ethylenediamine tetra-acetic acid (EDTA), 5 µg/mL aprotinin, 5 µg/mL leupeptin, 1% Triton X-100, 1% sodium deoxycholate, and 0.1% sodium dodecyl sulfate (SDS). The cell extract with 50 µg protein was loaded on a 10% or 15% SDS-polyacrylamide gel and then transferred to a nitrocellulose membrane. The membrane was incubated for 1 h in PBS-Tween 20 buffer containing 5% skim milk. After blotting with primary antibody, the protein expression was revealed with the appropriate horseradish peroxidase-labeled secondary antibody, which was detected using LumiGLO chemiluminescent substrate (Cell Signaling). Mouse anti-human β-tubulin was used as internal reference to ensure equal loadings.

In Vivo Treatment of Intracerebellar Xenografts with VPA

Balb/c nude (nu/nu) mice were obtained from the breeding facility at the animal center of Sun Yat-Sen University. All animal studies were performed in accordance with the institutional ethical guidelines for experimental animal care in the Cancer Center of Sun Yat-Sen University. To establish intracerebellar xenograft models, 4-week-old mice were anesthetized with sodium pentobarbital (50 mg/kg), after which a small skin incision (1 mm) was made and a burr hole (0.7 mm in diameter) was created with a microsurgical drill. U87MG cells (10⁵) were suspended in 2 µL of culture medium and injected slowly through the burr hole into the right cerebellar hemisphere (1 mm to the right of the midline, 1 mm posterior to the coronal suture, and 3 mm deep). The incision was closed with wound clips and removed 3 days after surgery.

Valproic acid was dissolved in 0.9% sodium chloride solution to a final concentration of 600 mg/mL. Valproic acid solution (400 mg/kg per day for 14 days) was administered by intraperitoneal injection.⁹ TMZ was administered at a dose of 40 mg/kg per day

(equivalent to 200 mg/m² in humans) for 5 days by oral gavage.¹⁸ PBS was used as negative control. Both treatments were started on Day 3 after the implantation of tumor cells. At the end of treatment, all mice were sacrificed. The mouse brains were removed and stored in liquid nitrogen overnight, then sectioned at 5- μ m thickness on a MicromHM200 cryotome (Eryostar). For immunohistochemical (IHC) analysis, mouse brain sections were fixed in 4% paraformaldehyde for 20 min, then permeated by 0.25% Triton X-100, and later immersed with the primary antibodies against MAP1-LC3 (1:200) overnight at 4°C. IHC was performed using the DAKO ABC System (Dako, Denmark). MAP1-LC3-positive cells were counted under 10 \times 40 high-power fields and expressed as percentage of total cells counted as described previously.¹⁹

Statistical Analysis

The data were expressed as mean \pm SD. Statistical analysis was performed using Student's *t*-test (two-tailed). The criterion for statistical significance was taken as *P* < .05.

Results

Effect of VPA on Malignant Glioma Cells

To examine the cytotoxicity of VPA on malignant glioma cells, we treated three malignant glioma cell lines (U87MG, T98G, and SF295) with VPA at concentrations ranging from 0.25 to 10 mM for 96 h. As shown in Fig. 1A, VPA increased cell death in all three cell lines in a dose-dependent manner, but their responses varied. IC₅₀ values for T98G, U87MG, and SF295 were 3.85 \pm 0.58, 2.15 \pm 0.38, and 6.16 \pm 0.84 mM, respectively. To investigate whether cell cycle arrest is induced in glioma cells by VPA, we performed DNA flow cytometric analyses. As shown in Fig. 1B, VPA treatment (1.0 mM, 96 h) increased the population at the G₀/G₁ phase and decreased the population at the S phase in all three tested glioma cell lines. These results indicate that VPA induces G₀/G₁ arrest in malignant glioma cell lines. The percentage of the sub-G₁ population, which is indicative of apoptosis, increased after treatment with VPA in T98G, U87MG, and SF295 cells: from 0.3% to 2.8% in T98G, from 0.4% to 7% in U87MG, and from 0.2% to 5% in SF295 cell lines, respectively.

VPA Induces Autophagy in Glioma Cells

To confirm the hypothesis that VPA can induce autophagy in glioma cells, we performed several analyses. Electron microscopic (EM) and GFP-LC3-labeling analyses showed that autophagic vacuoles increased in the U87MG cell line treated with 1.0 mM VPA for 96 h (Fig. 2A, B, and D). Most of the autophagosomes contained lamellar structures or residual digested

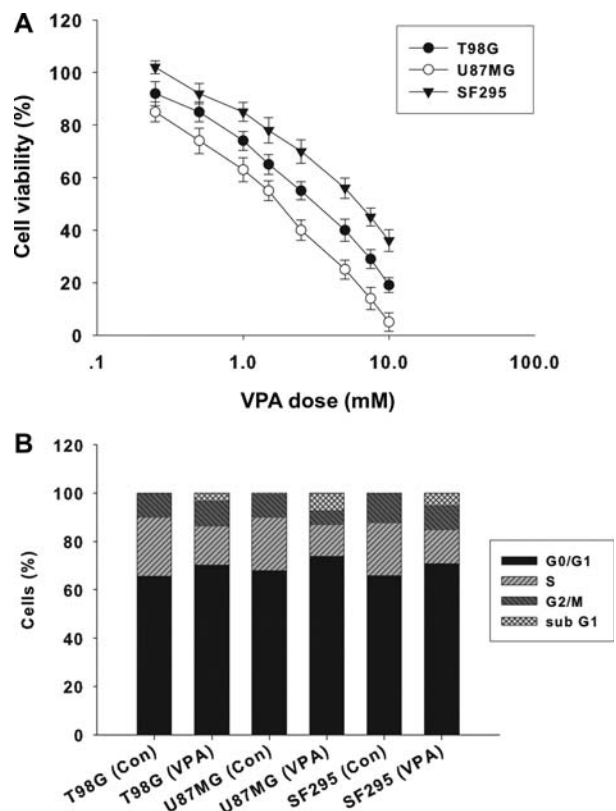


Fig. 1. Effect of VPA on malignant glioma cells. (A) Cytotoxic effect of VPA on U87MG, SF295, and T98G glioma cells for 96 h. The viability of the untreated cells was regarded as 100%. Points, mean of three independent experiments; bars, SD. (B) Effect of VPA on cell cycle in three glioma cell lines. After serum deprivation for 36 h, malignant glioma cells treated with or without VPA (1.0 mM) for 96 h were collected and stained with propidium iodide and analyzed in the FACScan. The percentage of cells in different phases of the cell cycle was determined using Cell Quest software.

components, whereas untreated tumor cells exhibited few such features (Fig. 2Aa and Ac).

To quantify the incidence of VPA-induced autophagy, we used MDC staining. All three glioma cell lines showed enhanced MDC-specific activities that increased after treatment with VPA in either a dose- or time-dependent manner (Fig. 2C and D). Moreover, addition of 3-MA inhibited the MDC incorporation after treatment with VPA (Fig. 2F).

In addition, we examined the expression of two MAP1-LC3 forms, LC3-I and LC3-II, using Western blot analysis, since LC3-II is closely associated with the membrane of autophagosomes.¹⁵ Expression of LC3-II increased in U87MG cell lines treated with VPA in a dose- or time-dependent manner (Fig. 2B). Similar results can also be observed for Beclin-1. GFP-LC3 staining also showed that addition of 3-MA decreased GFP-LC3-labeling cells after treatment with VPA (Fig. 2F). Combined with results revealed above, our data indicated that VPA induced autophagy in glioma cell lines.

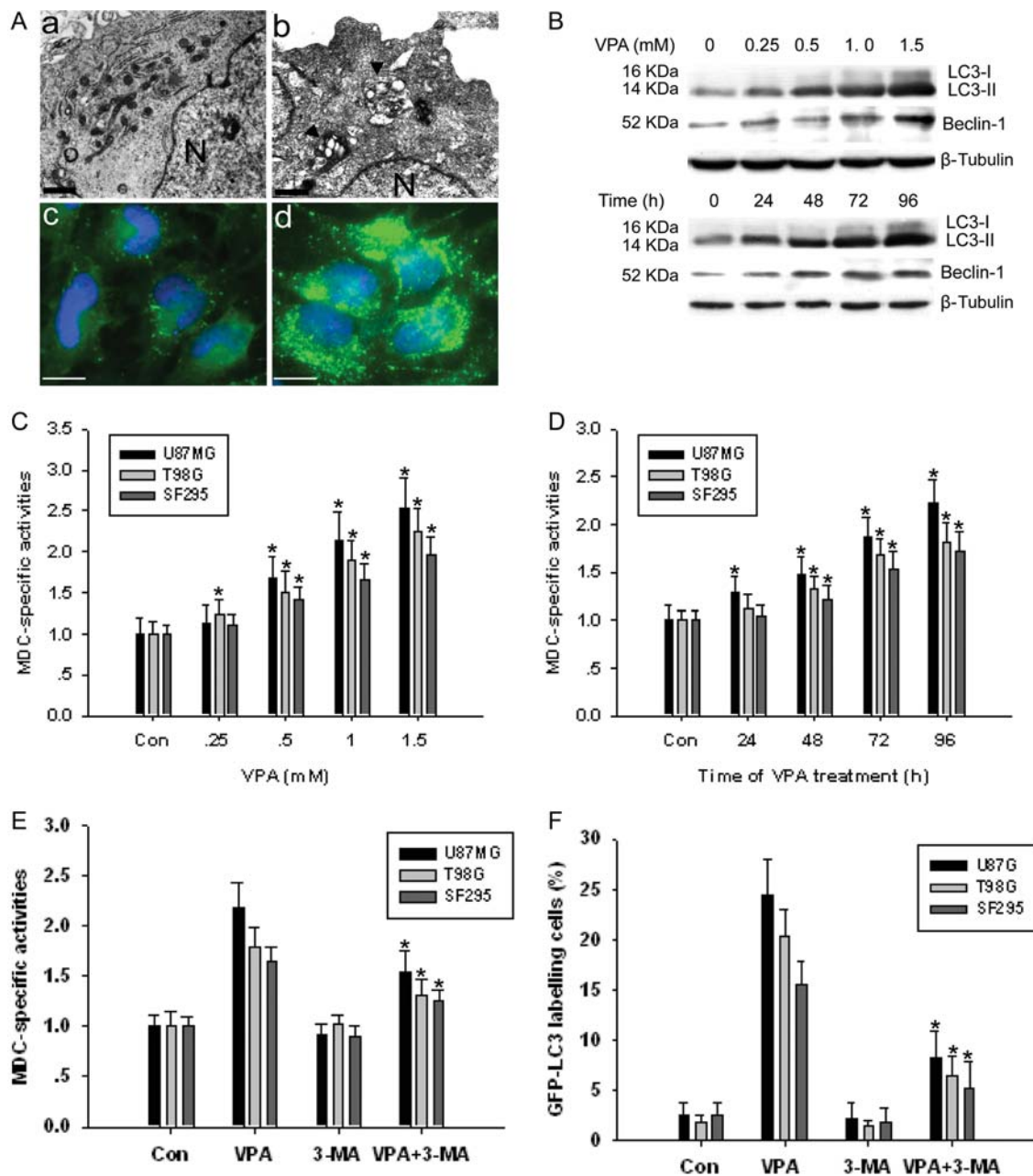


Fig. 2. (A) Ultrastructural features of VPA-induced autophagy in glioma cells. The cells treated with (1.0 mM) or without VPA for 96 h were harvested and fixed, and the electron microscopic observation was performed. GFP-LC3 plasmid was transfected into glioma cells 24 h before VPA treatment. (a and c) Untreated U87MG cells and (b and d) VPA-treated U87MG cells. N indicates nucleus. The arrowhead indicates autophagosome including residual digested material. Bar, a, b, 2.5 μm; c, d, 10 μm. (B) Representative Western blot showing MAP1-LC3 and Beclin-1 in U87MG cells before or after VPA exposure for dose (96 h) or for time study (1.0 mM). (C and D) MDC staining in glioma cells before or after VPA exposure for dose (96 h) or for time study (1.0 mM VPA). **P* < .05, as compared to noVPA control. (E) MDC-specific activities induced by VPA (1.0 mM, 96 h) can be suppressed by autophagy inhibitor 3-MA. **P* < .05, when compared with VPA-treated group. (F) The percentage of GFP-LC3-labeled cells in VPA group (1.0 mM, 96 h) can be reduced by autophagy inhibitor 3-MA. **P* < .05, when compared with VPA-treated group. Results shown are the means ± SD of three independent experiments.

Autophagy Is Crucial for VPA-Induced Cell Death

To further examine the role of autophagy in VPA-induced cell death, we performed Trypan blue

exclusion assay and annexin V-FITC staining. The pan-caspase inhibitor Z-VAD-fmk did not prevent cell death, indicating that caspase-independent death mechanisms might be triggered by VPA in these glioma cell lines.

Cell death induced by VPA can be significantly alleviated by autophagy inhibitor 3-MA (2.5 mM), whereas it was only slightly affected by Z-VAD-fmk, suggesting that autophagy, rather than apoptosis, is a crucial mechanism in the tumoricidal effect of VPA (Fig. 3A). Treatment with VPA (1.0 mM, 96 h) did not dramatically increase the percentage of annexin V-FITC-positive cells (Fig. 3B). Even in apoptosis-proficient U87MG cells that harbor wild-type p53 and functional caspase-3, the apoptosis rate was relatively low ($2.2 \pm 1.1\%$). In contrast, treatment with 5 μ M cisplatin for 48 h induced apoptosis in $17.7 \pm 2.6\%$, $13.5 \pm 2.8\%$, and $22.6 \pm 3.1\%$ of T98G, SF295, and U87MG cells, respectively. Apoptosis induced by VPA can be neutralized by caspase inhibitor Z-VAD-fmk, while not by autophagy inhibitor 3-MA, suggesting that apoptosis is independent of autophagy. Caspase-3 analysis showed similar results (Fig. 3C). Caspase-3 study also revealed

that activation of caspase-3 induced by VPA can be considerably enhanced by ERK1/2 inhibitor PD98059.

VPA-Induced Accumulation of Mitochondrial ROS, Loss of Membrane Potential, and Mitochondrial Injuries

To confirm the oxidative stress induced by VPA, we assessed the accumulation of ROS. Similar to other cell systems,¹⁷ VPA treatment for 96 h increased DCF fluorescence in all three cell lines (Fig. 4A). This effect can be suppressed by NAC, but not autophagy inhibitor 3-MA, indicating that ROS production occurs upstream of autophagy. In addition to being able to generate ROS, mitochondria are susceptible to damage by ROS. As shown in Fig. 4C and D, normal mitochondria existed in a cell as interconnected tubular networks that appear as a reticulum or as multiple individual punctate

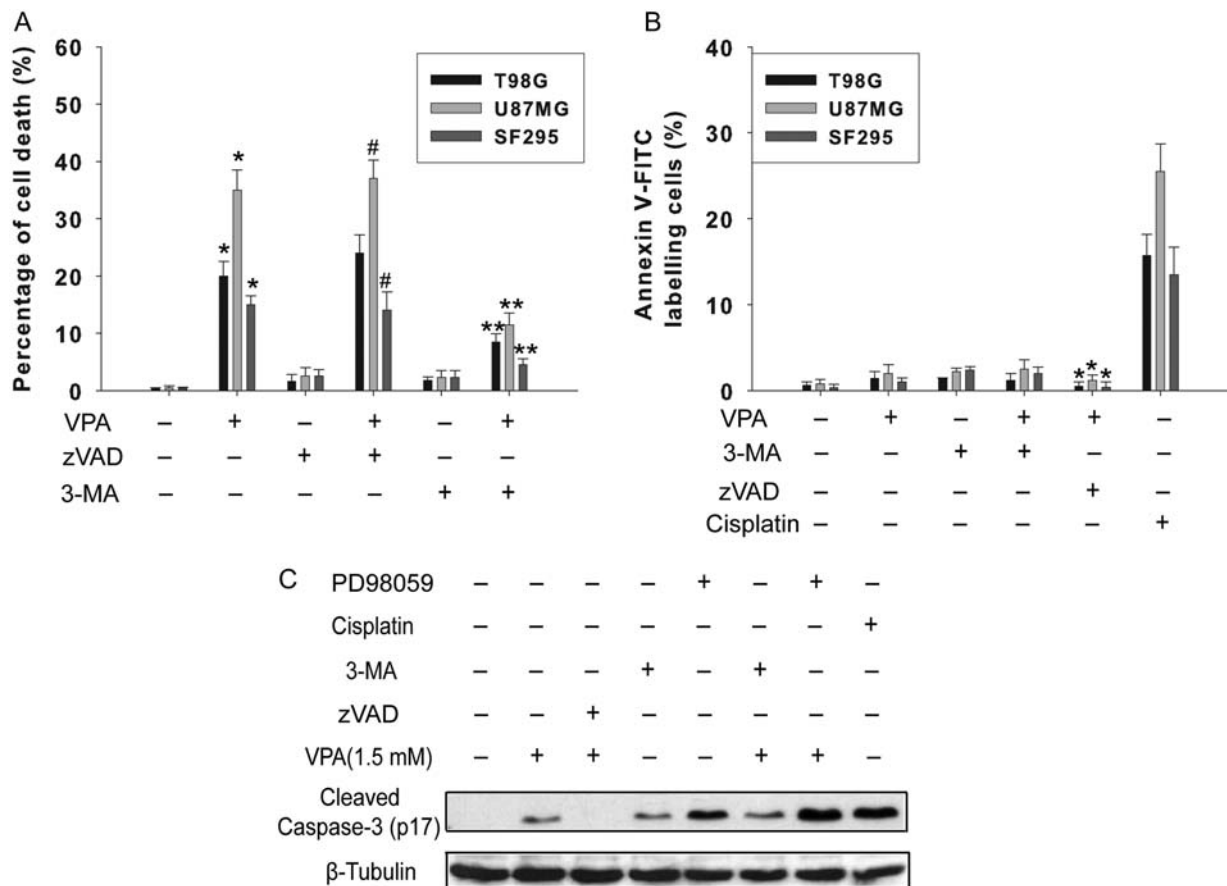


Fig. 3. Autophagy is crucial for VPA-induced cell death. Cells were seeded in 12-well plates at 2×10^4 per mL. At 48 h after exposure to VPA (1.0 mM), 3-MA (2.5 mM), zVAD (100 μ M), and PD98059 (10 μ M) were added and the cells were cultured for an additional 48 h. (A) Quantification of cell death after exposure to VPA alone or in combination. Cell death was determined by Trypan blue exclusion assay. * $P < .05$, as compared to noVPA group, ** $P < .05$, when compared with VPA-treated group. # $P > .05$, when compared with VPA-treated group. (B) Apoptosis detection in glioma cells treated with VPA alone or in combination with various drugs. After treatment, cells were labeled with annexin V-FITC, and counterstained with DAPI. Five hundred cells were analyzed for each sample. Cisplatin (5 μ M) was used as drug control for apoptosis. * $P < .05$, when compared with VPA-treated group. Results were the mean \pm SD of three independent experiments. (C) Representative Western blot showing cleaved caspase-3 (p17) in U87MG cells following exposure to 1.0 mM VPA alone or in combination with various drugs for 96 h. β -Tubulin was used as loading control.

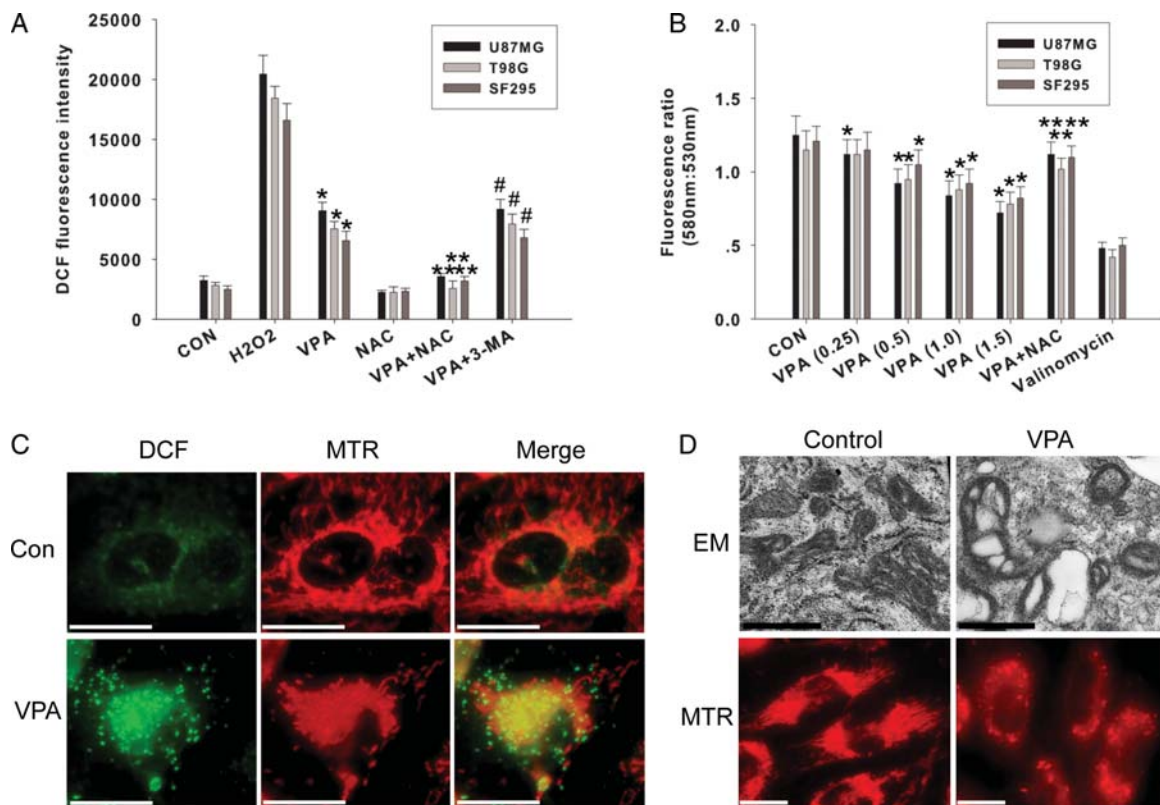


Fig. 4. Oxidative stress is an early event after exposure to VPA. (A) After pretreatment with NAC (5 mM) or 3-MA (2.5 mM) for 24 h in U87MG cells, VPA (1.0 mM) was added and cells were cultured for an additional 96 h. H₂O₂ (100 μ M, 6 h) was used as positive control. Intracellular oxidative stress was measured with DCF fluorescence intensity. * $P < .05$, as compared to noVPA group. ** $P < .05$, when compared with VPA-treated group. # $P > .05$, when compared with VPA-treated group. Data are presented as the mean \pm SD of three independent experiments. (B) Effects of VPA on MMP assessed by the JC-1 fluorescent probe. U87MG cells were treated with VPA (0.25, 0.5, 1.0, 1.5 mM) for up to 96 h valinomycin (10 mM) was used as positive control. NAC (5 mM) was added 24 h before VPA (1.0 mM) treatment. * $P < .05$, when compared with the nonVPA group. ** $P < .05$, when compared with VPA-treated group (1.0 mM). Values are expressed as mean \pm SD of three independent experiments. (C) Mitochondrial ROS generation in glioma cells after exposure to VPA. Representative fluorescent staining showing ROS visualized by DCF fluorescence (green), and mitochondria labeled by mitotracker red CMXRos (red) in U87MG cells yellow color indicates the colocalization between ROS and mitochondria. Bar, 10 μ m. (D) VPA treatment resulted in mitochondrial injuries. After exposure to VPA, U87MG cells were stained by mitotracker red CMXRos (MTR) or collected for electron microscopic analysis. Upper panel, bar, 1 μ m; lower panel, bar, 10 μ m.

organelles, while after VPA treatment (96 h), mitochondria exhibited swelling morphology, the reticular pattern was disrupted, and the number of cristae was also markedly reduced. All these results suggested that mitochondrial ROS induced by VPA might result in mitochondrial injury.

To examine the effect of VPA on mitochondrial function, the glioma cells were treated with JC-1. A loss in MMP has been indicated by a decrease in the red/green fluorescence intensity ratio. Valproic acid affected the MMP in all cell lines in a dose-dependent manner (0.25–1.5 mM) as compared to untreated controls (Fig. 4B). The positive control, potassium ionophore valinomycin, resulted in MMP depolarization as indicated by a 50%–60% decrease in the fluorescence intensity ratio following 15 min of treatment. A recovery in MMP was also observed in the cells treated with 5 mM NAC. Our data confirmed the role of mitochondrial ROS in VPA-induced mitochondrial dysfunction.

Autophagy Induced by VPA Is Regulated by Oxidative Stress

To confirm the hypothesis that autophagy induced by VPA is regulated by oxidative stress, we performed several analyses. As shown in Fig. 5A, cell death induced by VPA can be significantly alleviated by ROS scavenger NAC (5 mM), suggesting that oxidative stress is crucial for the tumoricidal effect of VPA. Similarly, NAC inhibited the increase of GFP-LC3 labeling cells after exposure to VPA. The addition of apoptosis inhibitor zVAD actually mildly enhanced autophagy induced by VPA, whereas inositol had no effect on VPA-induced autophagy, suggesting that autophagy is independent of apoptosis (Fig. 5B). Moreover, upregulation of LC3-II can be inhibited by NAC, 3-MA, and PD98059 in U87MG cell lines (Fig. 5D). MDC staining in all cell lines showed that addition of 3-MA, PD98059, and NAC inhibited the MDC incorporation after treatment with VPA (Fig. 5C), whereas inositol

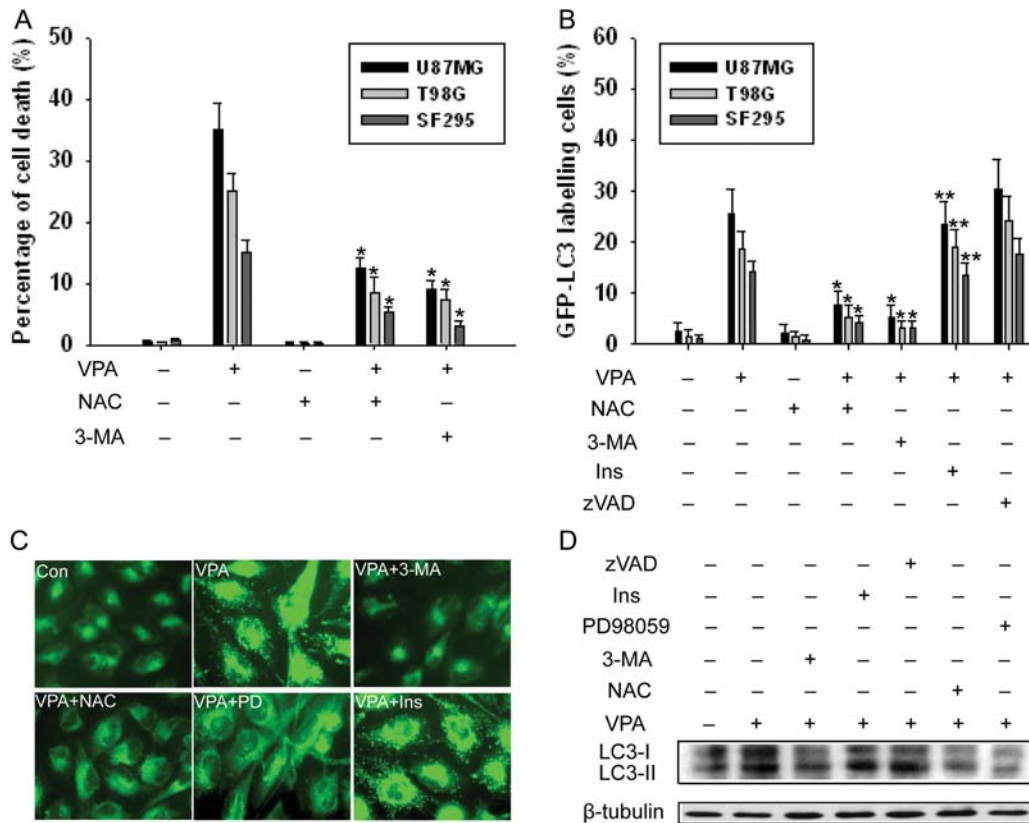


Fig. 5. VPA promotes autophagy through induction of oxidative stress. Cells were seeded in 12-well plates at 2×10^4 per mL. At 48 h after exposure to VPA (1.0 mM), 3-MA (2.5 mM), NAC (5 mM), zVAD (100 μ M), PD98059 (10 μ M), or inositol (1 mM) was added and cells were cultured for an additional 48 h. (A) Quantification of cell death after exposure to VPA alone or in combination. Cell death was determined by trypan blue exclusion assay. $*P < .05$, as compared to the VPA-treated group. (B) Quantification of cells expressing LC3 aggregation after VPA treatment. The percentage of LC3 aggregated cells was quantitated by counting the number of the cells showing the punctate pattern of GFP-LC3 in 200 GFP-positive cells. Results shown are the means \pm SD of three independent experiments. $*P < .05$, $**P > .05$, when compared with the VPA-treated group. (C) MDC staining in U87MG cells. Autophagosome was labeled by MDC (green punctuate), Magnification 400 \times . (D) Representative Western blot showing MAP1-LC3 in U87MG cells following exposure to 1.0 mM VPA alone or in combination with various drugs for 96 h. β -Tubulin was used as a loading control.

had no effect. Our data indicated that VPA induced autophagy in glioma cells, which was regulated by oxidative stress.

Role of the ERK Pathway in VPA-Induced Autophagy

Because the ERK pathway positively regulates autophagy in cancer cells,²⁰ we also examined this pathway. As examined by Western blot analysis, treatment with VPA for 24–96 h increased phosphorylated ERK1/2 (p-ERK1/2) in U87MG glioma cells (Fig. 6A). Immunofluorescence assay showed increased ERK 1/2 phosphorylation in the cells following VPA treatment for 96 h (Fig. 6D). The activation of ERK1/2 can be inhibited by PD98059 and NAC, suggesting the role of oxidative stress in its signaling regulation (Fig. 6A and D).

To determine whether activation of the ERK pathway is involved in VPA-induced autophagy, we used an MEK1 inhibitor, PD98059. Expression of LC3-II increased in the cells treated with VPA but decreased in the cells pretreated with PD98059 and then treated with VPA for 96 h

(Fig. 5D). We then determined the extent of the inhibitory effect of PD98059 on VPA-induced autophagy in glioma cell lines by examining GFP-LC3 localization. The percentage of cells with GFP-LC3 dots decreased significantly in the cells treated with PD98059 and VPA compared with VPA alone (Fig. 6C). The ERK pathway is known as an antiapoptosis pathway.²¹ Its inhibition by PD98059 enhanced apoptosis in VPA-treated cells (Figs. 3C and 6B). These results indicated that blocking the ERK pathway has a negative effect on the VPA effect, which suggests that the ERK pathway is involved in VPA-induced autophagy in glioma cells. ERK1/2 activation might constitute a mechanism through which oxidative stress regulates autophagy.

VPA Sensitized Glioma Cells to Phosphatidylinositol 3-Kinase or mTOR Inhibitor via Augmentation of Autophagy

Autophagy is activated mainly through the disruption of the PI3K/Akt/mTOR signaling pathway.⁷ Ly294002,

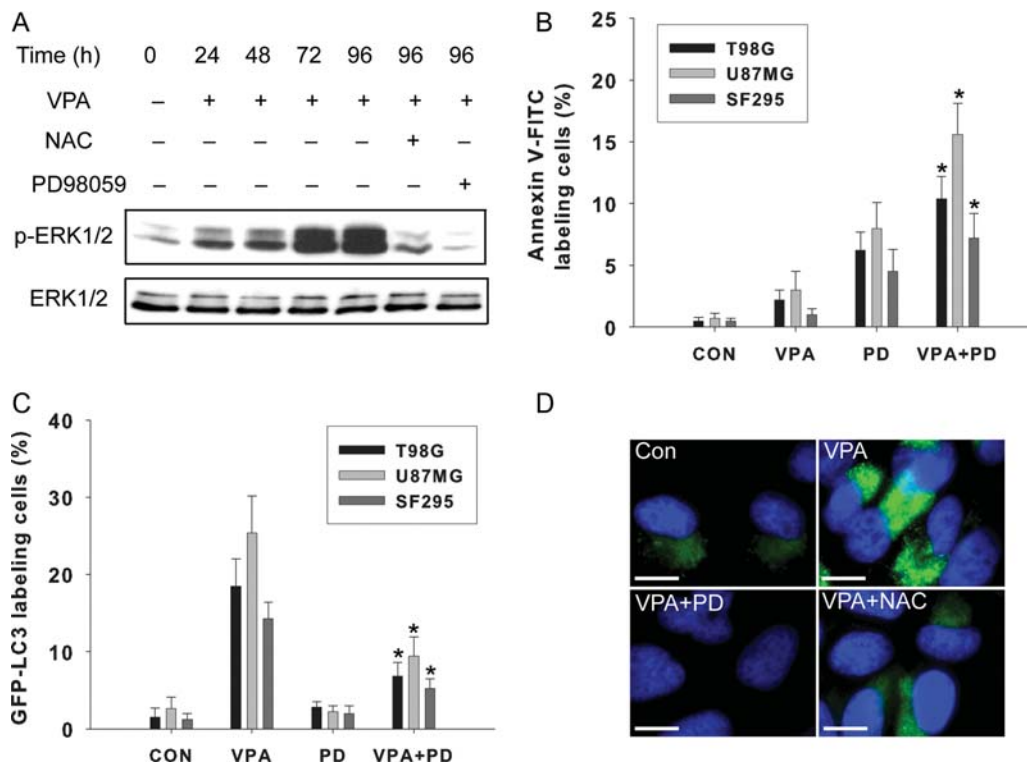


Fig. 6. Role of the ERK pathway in VPA-induced autophagy. (A) Representative Western blot showing ERK 1/2 phosphorylation in U87MG cells after treatment without (control) or with VPA (1.0 mM) alone for 24–96 h or with PD98059 (10 μM) or NAC (5 mM). (B) Apoptosis measured using annexin V-FITC staining. Cells were treated with 1.0 mM VPA alone or with 10 μM PD98059 for 96 h. Data were the mean of triplicate experiments; error bars, SD * $P < .05$, as compared to the VPA-treated group. (C) Quantitation of cells with GFP-LC3 dots among cells treated with 1.0 mM VPA alone or 1.0 mM VPA and 10 μM PD98059. Cells were transiently transfected with the GFP-LC3 plasmid for 24 h and then treated for 96 h as described. The number of cells with GFP-LC3 dots was counted, and their percentage among the total number of cells expressing GFP was determined. Data were the mean of triplicate experiments; error bars, SD * $P < .05$, when compared with the VPA-treated group. (D) Representative immunostaining of p-ERK1/2 in U87MG cells with VPA (1.0 mM) alone or with PD98059 (10 μM) and NAC (5 mM) for 96 h. Bar, 10 μm.

rapamycin, and TMZ are known inducers for autophagy in glioma cells.⁷ We determined the sensitivity of malignant glioma cells to these drugs alone or in combination with VPA based on cell viability (Fig. 7A). Our data showed that Ly294002, rapamycin, and TMZ combined with VPA increased cell death more than they did alone. To confirm that the combinatory interactions of these drugs with VPA could be attributed to the augmentation of autophagy, we performed MDC staining and annexin V-FITC staining. As shown in Fig. 7C, in U87MG, T98G, and SF295 cell lines, the combination treatment significantly increased MDC incorporation when compared with the single-agent treatment. However, VPA did not significantly enhance apoptotic cell death when combined with other autophagy inducers (Fig. 7B).

As shown in Fig. 7D, VPA enhanced TMZ-induced cytotoxicity in tested glioma cell lines. In T98G cells, IC₅₀ of TMZ plus VPA (1.0 or 1.5 mM) suppressed cell viability to <50% of that of TMZ alone. Kanzawa et al.⁵ reported that TMZ is an inducer for autophagy rather than for apoptosis in glioma cells. Therefore, our data may reflect the fact that the combined effects might depend on the stimulation of autophagic cell death.

VPA Induces Autophagic Cell Death in Intracerebellar Glioblastoma Xenografts

To assess the effect of VPA on U87MG intracerebellar glioblastoma xenografts, autophagic effect was examined by immunohistochemical staining of MAP1-LC3. In PBS-treated U87MG tumors, <10% of the tumor cells were MAP1-LC3 positive, and treatment with VPA caused a significant increase of MAP1-LC3 expression (Fig. 8A; $P < .05$). In contrast to either VPA or TMZ alone, treatment with the drug combination significantly increased the percentage of MAP1-LC3-expressing cells in U87MG tumors (Fig. 8A; $P < .05$). Increases in necrotic cell with MAP1-LC3 staining were observed in all three drug-treated groups, and the combination of TMZ with VPA exhibited the highest level of autophagy-related cell death (Fig. 8B). These results suggest that cell death induced by VPA alone or in combination with TMZ is correlated with the induction of autophagy.

Discussion

Valproic acid, a commonly used drug for treating epilepsy and bipolar disorders, has emerged as a promising

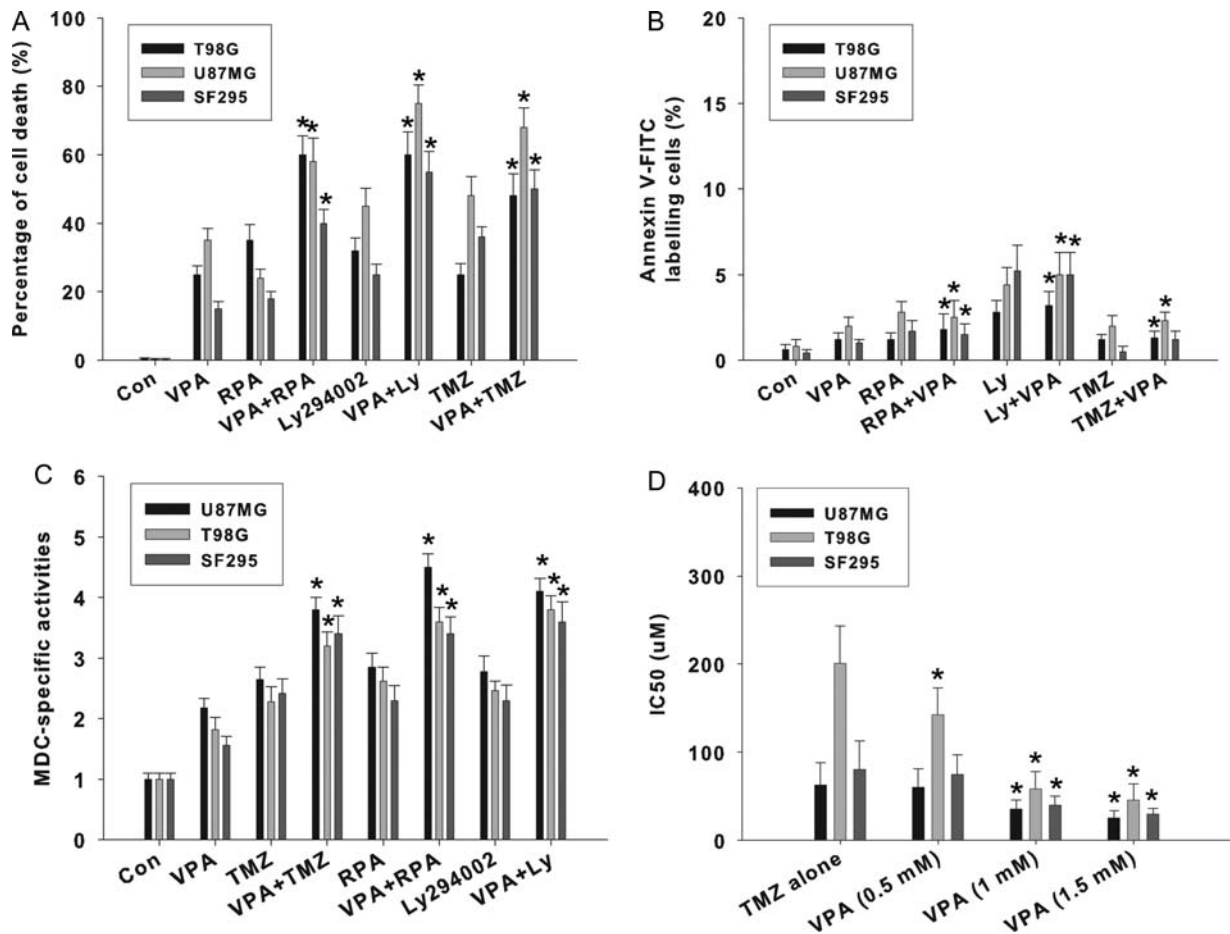


Fig. 7. VPA potentiates autophagic cell death when combined with other autophagy inducers. VPA potentiates autophagic cell death when combined with TMZ, rapamycin (RPA), or Ly294002 (Ly). Cells were treated with 1.0 mM VPA alone or in combination with TMZ (25 μ M), RPA (10 nM), or Ly294002 (1 μ M) for 96 h. (A) Trypan blue exclusion assay was used to evaluate cell death after drug treatment. * $P < .05$, as compared to TMZ, RPA, or Ly alone. (B) Apoptosis detection in U87MG and T98G glioma cells treated with VPA alone or in combination with TMZ, RPA, or Ly294002. After annexin V-FITC staining, 500 cells were analyzed for each sample. * $P > .05$, when compared with TMZ, RPA, or Ly294002 alone. (C) Quantitation of autophagic cells with MDC incorporation among cells treated with 1.0 mM VPA alone or in combination with TMZ, RPA, or Ly294002 for 96 h. * $P < .05$, when compared with TMZ, RPA, or Ly294002 alone. (D) VPA enhances TMZ-induced cytotoxicity. For cocubation experiments, a single concentration of VPA (0.5, 1.0, or 1.5 mM) and different concentrations of TMZ were added to cells and incubations carried out for 96 h. The viability of untreated cells was regarded as 100%. The IC₅₀ value was calculated with SPSS 10.0 statistical software. Data are the mean of triplicate experiments; error bars, SD * $P < .05$, when compared with TMZ alone (no VPA).

agent for cancer treatment in recent years.⁸ In addition to clinical assessment, the experimental examination of VPA as anticancer drug is ongoing, even though many questions regarding its underlying mechanisms remain poorly understood. Our present results indicated that VPA can induce autophagy, which constitutes the main cause of cell death instead of apoptosis in glioma cell lines. Even in apoptosis-proficient U87MG cells that harbor wild-type p53 and functional caspase-3, most of the cell death can be attributed to autophagy. Thus, following VPA treatment, glioma cells may die from a caspase-independent autophagic process showing signs of apoptosis, suggesting that cells may choose between the autophagic and the apoptotic execution pathways. Moreover, several experiments showed that the limits between apoptosis and autophagy may be tenuous and

suggest either considerable overlap or interdependence of both programs of cell demise.²² On a molecular level, this means that the apoptotic and autophagic response machineries share common pathways that either link or polarize the cellular responses.²²

Mitochondria produce low levels of ROS as an inevitable consequence of oxidative metabolism, thus generating the MMP that drives the synthesis of ATP by the F₁F₀-ATPase and almost all other mitochondrial functions.²³ While under oxidative stress, ROS are generated at higher levels, inducing cellular damage and cell death.²³ Cancer cells produce higher levels of ROS than normal cells because of increased metabolic stress and proliferative capacity, and thus may be more sensitive to oxidative stress as a result of high endogenous ROS levels and may provide a selective mechanism to

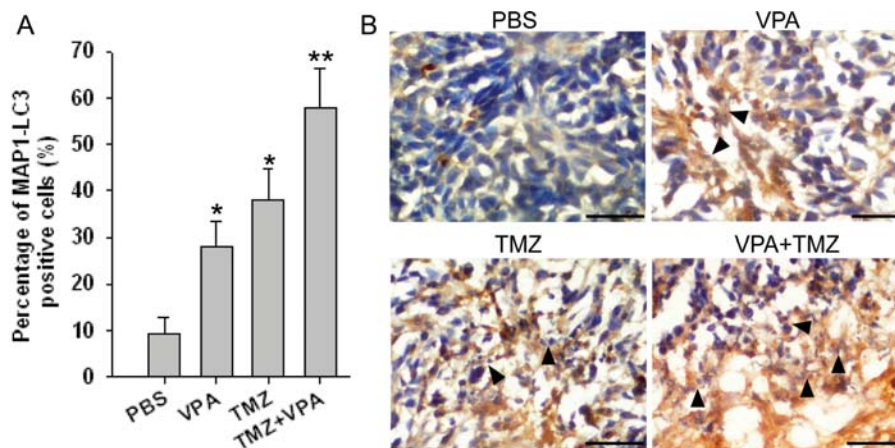


Fig. 8. VPA induces autophagy-related death in U87MG intracerebellar xenografts. Mice bearing intracerebellar xenografts were killed at the end of drug treatment and compared with the untreated group. (A) The number of cells identified by immunohistochemical staining with MAP1-LC3 were counted in digitally captured images under high-power (10×40) magnification and graphed as the percentage of total cells. Columns, mean; bars, SE. * $P < .05$, as compared to the PBS group ($n = 4$); ** $P < .05$, when compared with single drug ($n = 4$). (B) Induction of autophagy in necrotic cells after drug treatment. Necrotic cells were stained with MAP1-LC3 antibody. Black arrow head indicates the site of necrotic cells with MAP1-LC3 staining. Bar, 100 μm .

induce cell death.²⁴ In this study, we demonstrated that VPA is capable of producing elevated levels of mitochondrial ROS in glioma cells. ROS induced by VPA lead to loss of MMP and mitochondrial injuries in glioma cells, which cause cytotoxicity and ultimately cell death.

Several studies implicated mitochondrial ROS in the induction of autophagy.^{24,25} Cancer cells have an antioxidant system where antioxidant enzymes such as manganese-superoxide dismutase (SOD), catalase, and glutathione peroxidase eliminate ROS.²³ Chen et al.²⁴ recently reported that oxidative stress induced by H_2O_2 or SOD inhibitor 2-methoxyestradiol (2-ME) can cause autophagic cell death in transformed cell line HEK293, and cancer cell lines U87 and HeLa. Similarly, our data also indicated that autophagy induced by VPA is dependent on oxidative stress, suggesting that oxidative stress occurs upstream of autophagy. Therefore, our results may propose a central role for mitochondria as the source for redox regulation of autophagy after exposure to VPA in glioma cells. However, is the regulation of autophagy limited to mitochondria ROS production alone? Scherz-Shouval et al.²⁶ discovered redox as a posttranslational modification that regulates autophagy through the regulation of autophagy effector Atg4. In this study, we found that ERK1/2 activation was also regulated by oxidative stress.

Upregulation of ERK1/2 activity via enhanced activity of the *ras/raf-1/MEK/ERK* pathway is imperative for induction of autophagy in HT-29 colon cancer cells.²⁷ Lee et al.²⁸ showed that H_2O_2 treatment resulted in marked sustained activation of ERK, which can be prevented by catalase, the hydrogen peroxide scavenger. ERK2 knockdown by siRNA leads to collapse of MMP with acute oxidative stress in human lens epithelial cells.²⁹ Some evidence exists that the ERK pathway mediates apoptosis via the upstream action of mitochondrial

cytochrome *c* release and caspase-3 activation through upregulation of Bax and p53.³⁰ Our data actually revealed an opposite role of ERK in VPA-induced apoptosis, since its inhibition by PD98059 led to enhanced apoptosis. Thus, ERK1/2 activation might play a pivotal role in switching to oxidative stress-induced autophagy rather than apoptosis in glioma cells.

Recently, Sarkar et al.³¹ proposed that lithium induced autophagy via inositol monophosphatase (IMPase) inhibition, leading to free inositol depletion and reduced myo-inositol-1,4,5-triphosphate (IP3) levels. This represents a novel way of regulating mammalian autophagy, independent of the mTOR. Although inositol depletion is a first event shown to be common to lithium and VPA, VPA did not demonstrate any direct stimulation or inhibition on partially purified IMPase preparation derived from bovine brain, suggesting that reduced IP3 levels might be caused by other mechanisms.³² Nevertheless, our data also showed that addition of inositol did not attenuate autophagy induced by VPA, suggesting a different mechanism from that of lithium.

In summary, in the present study, we have demonstrated, for the first time, that VPA induced autophagy in malignant glioma cells through modulating oxidative stress. ERK1/2 activation is also required for induction of autophagy mediated by oxidative stress. In addition, a previous study indicated that autophagy failed to be significantly induced in primary astrocytes under oxidative stress.²⁴ Thus, targeting ROS generation could selectively induce autophagic cell death in cancer cells. This may lead to new strategies to develop therapeutic drugs that will selectively target cancer cells to undergo autophagy, inducing cell death independent of apoptosis. We also found that treatment combining temozolomide or rapamycin with VPA had a synergistic effect on development of autophagy in these glioma cell

lines, which may provide a promising rationale for using therapies that combine VPA and other proautophagic drugs for the treatment of patients with apoptosis-resistant gliomas. Recently, clinical trials have been conducted to determine the safety, toxicity, and maximum tolerated dose of VPA alone or in combination in solid tumor malignancies and to define its clinical feasibility.^{33,34} Thus, VPA could be a drug that could eventually be used in combination therapies, with classical cytotoxics, proautophagic drugs, or radiation, in gliomas.

Funding

This research was supported by the National Natural Science Foundation of China (No. 30772551) and State Key Laboratory for Cancer Research in Southern China Grant 985-II.

Conflict of interest statement. None declared.

References

1. Surawicz TS, Davis F, Freels S, et al. Brain tumor survival: results from the National Cancer Data Base. *J Neurooncol.* 1998;40:151–160.
2. Lefranc F, Facchini V, Kiss R. Proautophagic drugs: a novel means to combat apoptosis-resistant cancers, with a special emphasis on glioblastomas. *Oncologist.* 2007;12:1395–1403.
3. Kondo Y, Kanzawa T, Sawaya R, et al. The role of autophagy in cancer development and response to therapy. *Nat Rev Cancer.* 2005;5:726–734.
4. Hippert MM, O'Toole PS, Thorburn A. Autophagy in cancer: good, bad, or both? *Cancer Res.* 2006;66:9349–9351.
5. Kanzawa T, Germano IM, Komata T, et al. Role of autophagy in temozolomide-induced cytotoxicity for malignant glioma cells. *Cell Death Differ.* 2004;11:448–457.
6. Stupp R, Mason WP, van den Bent MJ, et al. Radiotherapy plus concomitant and adjuvant temozolomide for glioblastoma. *N Engl J Med.* 2005;352:987–996.
7. Takeuchi H, Kondo Y, Fujiwara K, et al. Synergistic augmentation of rapamycin-induced autophagy in malignant glioma cells by phosphatidylinositol 3-kinase/protein kinase B inhibitors. *Cancer Res.* 2005;65:3336–3346.
8. Michaelis M, Doerr HW, Cinatl J, Jr. Valproic acid as anti-cancer drug. *Curr Pharm Des.* 2007;13:3378–3393.
9. Li XN, Shu Q, Su JM, et al. Valproic acid induces growth arrest, apoptosis, and senescence in medulloblastomas by increasing histone hyperacetylation and regulating expression of p21Cip1, CDK4, and CMYC. *Mol Cancer Ther.* 2005;4:1912–1922.
10. Kamitani H, Taniura S, Watanabe K, et al. Histone acetylation may suppress human glioma cell proliferation when p21 WAF/Cip1 and gelsolin are induced. *Neuro-Oncology.* 2002;4:95–101.
11. Das CM, Aguilera D, Vasquez H, et al. Valproic acid induces p21 and topoisomerase-II (alpha/beta) expression and synergistically enhances etoposide cytotoxicity in human glioblastoma cell lines. *J Neurooncol.* 2007;85:159–170.
12. Schwartz C, Palissot V, Aouali N, et al. Valproic acid induces non-apoptotic cell death mechanisms in multiple myeloma cell lines. *Int J Oncol.* 2007;30:573–582.
13. Pan T, Li X, Xie W, et al. Valproic acid-mediated Hsp70 induction and anti-apoptotic neuroprotection in SH-SY5Y cells. *FEBS Lett.* 2005;579:6716–6720.
14. Michaelis M, Suhan T, Michaelis UR, et al. Valproic acid induces extracellular signal-regulated kinase 1/2 activation and inhibits apoptosis in endothelial cells. *Cell Death Differ.* 2006;13:446–453.
15. Jackson WT, Giddings TH, Jr, Taylor MP, et al. Subversion of cellular autophagosomal machinery by RNA viruses. *PLoS Biol.* 2005;3:861–871.
16. Munafó DB, Colombo MI. A novel assay to study autophagy: regulation of autophagosome vacuole size by amino acid deprivation. *J Cell Sci.* 2001;114:3619–3629.
17. Tong V, Teng XW, Chang TK, et al. Valproic acid II: effects on oxidative stress, mitochondrial membrane potential, and cytotoxicity in glutathione-depleted rat hepatocytes. *Toxicol Sci.* 2005;86:436–443.
18. Mathieu V, De Nève N, Le Mercier M, et al. Combining bevacizumab with temozolomide increases the antitumor efficacy of temozolomide in a human glioblastoma orthotopic xenograft model. *Neoplasia.* 2008;10:1383–1392.
19. Shu Q, Antalffy B, Su JM, et al. Valproic acid prolongs survival time of severe combined immunodeficient mice bearing intracerebellar orthotopic medulloblastoma xenografts. *Clin Cancer Res.* 2006;12:4687–4694.
20. Pattingre S, Bauvy C, Codogno P. Amino acids interfere with the ERK1/2-dependent control of macroautophagy by controlling the activation of Raf-1 in human colon cancer HT-29 cells. *J Biol Chem.* 2003;278:16667–16674.
21. Xia Z, Dickens M, Raingeaud J, et al. Opposing effects of ERK and JNK-p38 MAP kinases on apoptosis. *Science.* 1995;270:1326–1331.
22. Assunção Guimarães C, Linden R. Programmed cell deaths: apoptosis and alternative deathstyles. *Eur J Biochem.* 2004;271:1638–1650.
23. Scherz-Shouval R, Elazar Z. ROS, mitochondria and the regulation of autophagy. *Trends Cell Biol.* 2007;17:422–427.
24. Chen Y, McMillan-Ward E, Kong J, et al. Oxidative stress induces autophagic cell death independent of apoptosis in transformed and cancer cells. *Cell Death Differ.* 2008;15:171–182.
25. Chen Y, McMillan-Ward E, Kong J, et al. Mitochondrial electron-transport-chain inhibitors of complexes I and II induce autophagic cell death mediated by reactive oxygen species. *J Cell Sci.* 2007;120:4155–4166.
26. Scherz-Shouval R, Shvets E, Fass E, et al. Reactive oxygen species are essential for autophagy and specifically regulate the activity of Atg4. *EMBO J.* 2007;26:1749–1760.
27. Ogier-Denis E, Pattingre S, El Benna J, et al. Erk1/2-dependent phosphorylation of Galpha-interacting protein stimulates its GTPase accelerating activity and autophagy in human colon cancer cells. *J Biol Chem.* 2000;275:39090–39095.
28. Lee WC, Choi CH, Cha SH, et al. Role of ERK in hydrogen peroxide-induced cell death of human glioma cells. *Neurochem Res.* 2005;30:263–270.
29. Flynn JM, Lannigan DA, Clark DE, et al. RNA suppression of ERK2 leads to collapse of mitochondrial membrane potential with acute oxidative stress in human lens epithelial cells. *Am J Physiol Endocrinol Metab.* 2008;294:E589–E599.

30. Zhuang S, Schnellmann RG. A death-promoting role for extracellular signal-regulated kinase. *J Pharmacol Exp Ther*. 2006;319:991–997.
31. Sarkar S, Floto RA, Berger Z, et al. Lithium induces autophagy by inhibiting inositol monophosphatase. *J Cell Biol*. 2005;170:1101–1111.
32. Vadnal R, Parthasarathy R. Myo-inositol monophosphatase: diverse effects of lithium, carbamazepine, and valproate. *Neuropsychopharmacology*. 1995;12:277–285.
33. Atmaca A, Al-Batran SE, Maurer A, et al. Valproic acid (VPA) in patients with refractory advanced cancer: a dose escalating phase I clinical trial. *Br J Cancer*. 2007;97:177–182.
34. Münster P, Marchion D, Bicaku E, et al. Phase I trial of histone deacetylase inhibition by valproic acid followed by the topoisomerase II inhibitor epirubicin in advanced solid tumors: a clinical and translational study. *J Clin Oncol*. 2007;25:1979–1985.